IEEE Access
Multidisciplinary | Rapid Review | Open Access Journal

IEEE MAGNETICS SOCIETY SECTION

Received April 16, 2021, accepted April 30, 2021, date of publication May 10, 2021, date of current version May 18, 2021.

Digital Object Identifier 10.1109/ACCESS.2021.3078461

Open-Circuit Core Loss of Large Turbine Generators Considering the Influence of Key Bar Design

DAE-IL SONG[1,2], JUNGHWAN AHN[2], YOUNG-JOON NAM[1], JU LEE[1], (Senior Member, IEEE), AND HYUNGKWAN JANG[1]

[1]Department of Electrical Engineering, Hanyang University, Seoul 34056, Republic of Korea
[2]Korea Electric Power Research Institute, Daejeon 34056, Republic of Korea

Corresponding author: Hyungkwan Jang (jhkinhyu@hanyang.ac.kr)

This work was supported in part by the Korea Electric Power Corporation (KEPCO), and in part by the Tenaga Nasional Berhad (TNB) through the Project entitled by Creep Test of P91 Pipe Weldment under Grant R21GH01.

ABSTRACT To provide power to electrical power distribution systems cost effectively, it is necessary to understand the efficiency of large turbine generators. Stator cores, which account for 10%–15% of total generator losses, are supported by a either a dovetail key bar or a square key bar. The dovetail key bar, mainly used in large turbine generators, has a shallow depth of penetration into the stator core; consequently, the need for research related to core loss has been limited in the case of dovetail key bars. By contrast, the square key bar, which is attracting attention owing to its ease of assembly, deeply penetrates the stator core, and thus has a greater effect on core loss than the dovetail key bar. However, core losses due to the key bar design have not been examined quantitatively in the literature. This paper analyzes the core-loss changes due to the key bar. Using electromagnetic finite-element analysis, we calculate the differences in core loss between the two aforenoted key bar types, which are commonly used in large turbine generators. In addition, we propose points for consideration when designing key bars for large-capacity generators.

INDEX TERMS Core loss, magnetic flux density, finite-element analysis (FEA), key bar, large turbine generator.

I. INTRODUCTION

Stable power generation is required to maintain electrical power-transmission systems that supply the baseload power needed for homes, hospitals, and factories.

Solar power and wind power have recently been spotlighted as representative sources of renewable energy. However, these energy sources are notably unstable and unreliable as they are highly dependent on the weather. Therefore, reliable thermal and nuclear power plants remain important and relevant for complementing developing renewable energy sources.

Unlike other rotating machinery, turbine generators located in power plants are characterized by a large capacity and long continuous-operation time. The capacity of a turbine generator in a power plant is typically between 100 and 1,000 MW [1]–[3]. The lifetime of a generator exceeds 20 years, and generators operate continuously during their lifetime [4], [25]. Because the energy costs of generating electricity are directly proportional to the work applied to the generator, a difference of even 1% in efficiency will have a significant economic impact over the operational lifetime of a generator. Therefore, to supply the exact power required by electrical power distribution systems and to predict the economics of power plants, it is important to identify the generator losses correctly. Owing to the development of computer technology, many studies now utilize finite-element analysis (FEA) to accurately predict the losses arising from large generators [6]–[14].

The loss distribution of a large turbine generator is shown in Fig. 1 [6]. The core loss occurs in the stator core; it is caused by the alternating magnetic flux that produces the generator voltage.

Depending on the type of generator, the core loss accounts for 10%–15% of the total losses. Since core loss is a major loss component in electric machineries, many studies

The associate editor coordinating the review of this manuscript and approving it for publication was Montserrat Rivas.

TABLE 1. Previous studies on core loss and key bar in large generators.

	Subject of study	Outcome (➢) / Feature (✧)	Ref.
Core loss	Calculation of the core loss	➢ Core loss of the generator ✧ No consideration of the key bar design	[22]–[24]
Key bar	Detection of stator core fault	➢ Fault current through the key bar and stator core ✧ Dovetail key bar–type generator ✧ No report on the core loss	[25]–[27]
	Key bar voltage in the open-circuit condition	➢ Key bar voltage according to generator terminal voltage ✧ Dovetail key bar–type generator ✧ No report on the core loss	[28]

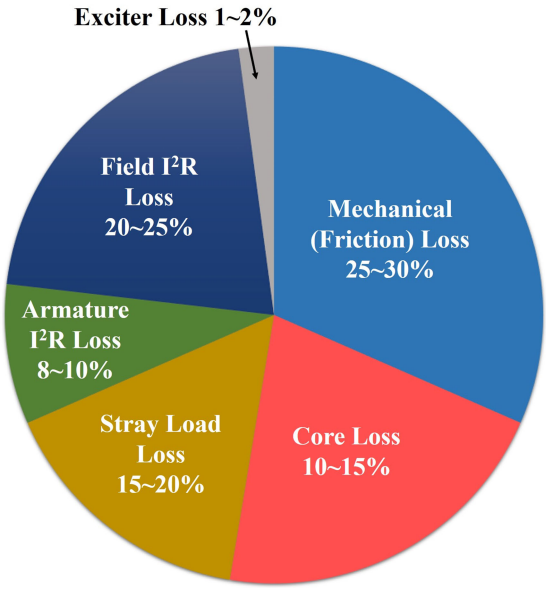

FIGURE 1. Loss distribution of a large turbine generator.

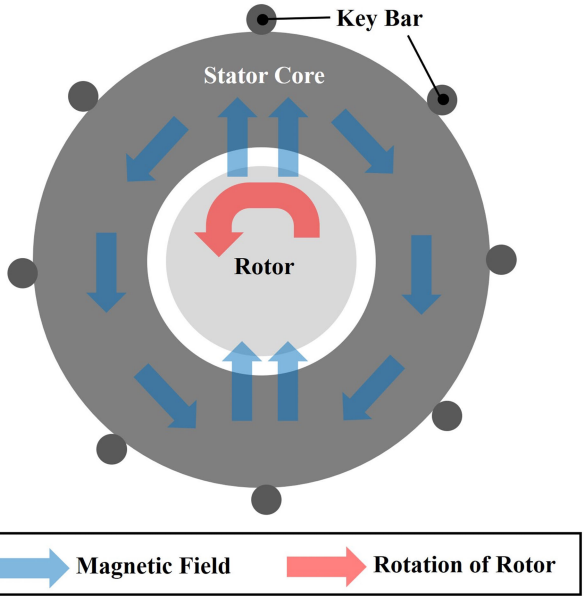

FIGURE 2. Location of the key bar in a large turbine generator.

have reported on calculation formulas or models for core loss [15]–[17]. General power loss properties of soft ferromagnetic materials have been studied [15], resulting in an improved equation for lamination core loss [16] and a core loss model for soft ferromagnetic materials [17]. Further, core loss in energy-conversion devices has been reported [18]–[24]. By applying FEA, the core losses of a motor [18]–[21], synchronous generator [22], [23], and hydropower generator were accurately calculated [24].

The rotating magnetic field inside a generator exerts forces on the stator core, which could cause it to move. As shown in Fig. 2, the key bar supports the stator core firmly during operation, preventing any movement. To achieve core stability, part of the key bar must penetrate the stator core, but this can lead to increased core-efficiency losses. The depth of core penetration (and thus the core loss) depends on the type of key bar employed.

Dovetail key bars, which are mainly used in large turbine generators, entail shallow penetration into the stator core. Their effect on core loss is small enough to be neglected; consequently, the need for research regarding core loss when considering a dovetail key bar is minimal. For dovetail key bars, the current due to stator core fault [25]–[27] and the key bar voltage [28] have been reported. However, square key bars, which are increasingly attracting attention due to their ease of assembly, penetrate deeply into the stator core, and their effect on core loss is consequently greater than that of dovetail key bars. Nevertheless, as shown in Table 1, to the best of our knowledge, there are no published studies on core loss considering the influence of key bar design.

In this paper, we elucidate the influence of key bars on core loss. We studied two types of key bars that are frequently used in large-turbine-generator design. We conducted FEA to calculate the core loss and performed factory t tests to verify the computational results. At the end of the paper, we suggest points for consideration when designing the key bar for an electrical generator.

II. THEORY

A. OPEN-CIRCUIT CORE LOSS

Inside the generator, the mechanical power from a turbine, determined by the product of the rotating speed and torque, is converted into electrical power, defined as the product of voltage (V), current (I), and power factor ($\cos\theta$):

$$Torque \cdot Speed = V \cdot I \cdot \cos\theta \tag{1}$$

Large turbine generators are connected to the electrical power grid and transmit electrical power. To transfer electrical power to the electrical power grid, the voltage in (1) must be kept constant. The voltage is defined as

$$V = K_p \cdot K_d \cdot \sqrt{2}\pi f \cdot \phi \cdot N_{atckt} \tag{2}$$

where V is the terminal voltage of the generator, N_{atckt} is the number of armature winding turns, f is the operating frequency, and K_p and K_d are the armature winding pitch factor and armature winding distribution factor, respectively. The magnetic flux ϕ in the generator is related to the magnetic flux density B_C in the stator core as follows:

$$B_C = K_S \cdot \frac{\phi}{L_{SC} \cdot W_{SC}} \tag{3}$$

where K_S is a coefficient determined by the ratio of magnetic to non-magnetic materials such as insulation throughout the stator core, and L_{SC} and W_{SC} are the length and width of the stator core, respectively. In an AC power system, the magnetic flux passes through the stator core at 60 Hz. This alternating magnetic flux causes the core loss in the stator core, which is defined [16], [17] as follows:

$$\begin{aligned} P_{Core\ Loss} &= P_E + P_H + P_A \\ &= K_E \cdot B_C^2 \cdot f^2 + K_H \cdot B_C^n \cdot f + K_A \cdot B_C^{1.5} \cdot f^{1.5} \end{aligned} \tag{4}$$

The core loss ($P_{Core\ Loss}$) consists of the eddy-current loss (P_E), hysteresis loss (P_H), and the excess loss (P_A). K_E, K_H, and K_A are the coefficients of the eddy-current loss, the hysteresis loss, and the excess loss, respectively. B_C is the magnetic flux density in the stator core, f is the operating frequency, and n is the exponent coefficient of the hysteresis loss. K_E, K_H, K_A, and n are material dependent.

In general, when designing an electrical generator, the core loss is calculated assuming that the magnetic flux density is distributed on the outer area of the stator core. However, when considering the key bar, the distribution of the magnetic flux density (B_C) in the stator core can be changed, particularly when using a square key bar. Therefore, the area where the key bars penetrate the stator core needs to be considered in detail, as shown in Fig. 3.

B. KEY BAR

The eddy-current loss of the stator core is proportional to the square of the core thickness [15]–[17]. Hence, thin steel plates are used for manufacturing stator cores, and hundreds of thousands to millions of plates are required, depending on the generator capacity. To support the stator core, dovetail and square key bars are used in large turbine generators, as shown in Fig. 3.

The dovetail key bar, Fig. 3(a), is designed to be wider toward the interior of the generator in order to support the stator core firmly. Only a small penetration depth is required when assembling the stator core and key bar. However, the assembly entails a considerable amount of time as it must be performed in the axial direction.

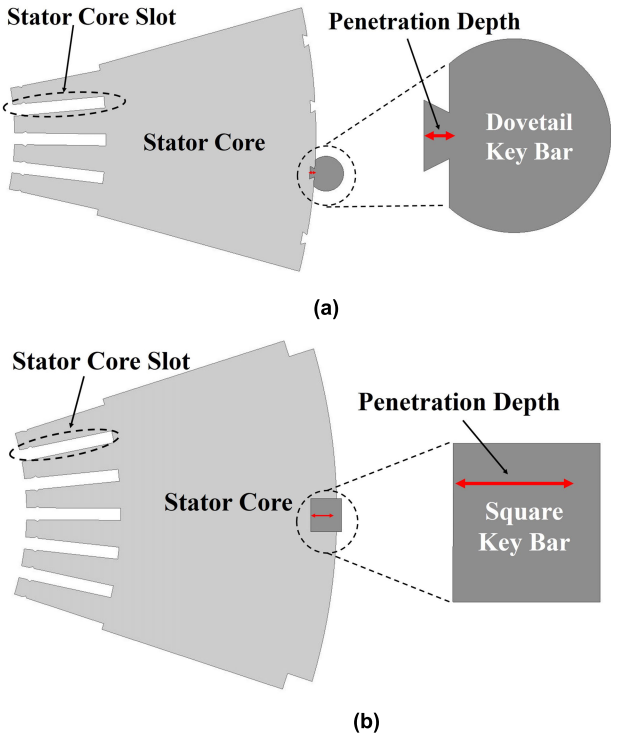

FIGURE 3. Stator core and key bar: (a) Dovetail key bar, (b) Square key bar.

TABLE 2. Generator specification.

	Dovetail type	Square type	Unit
Capacity	197	203	MVA
Power factor	0.9	0.9	PF
Output	177.3	182.7	MW
Core outer dimeter	2.4	2.4	meter
No. of poles	2	2	Each
Line voltage	15	15	kV
Line current	7,583	7,813	A
Speed	3,600	3,600	RPM
Cooling type	Air-cooled	Air-cooled	

The square key bar, shown in Fig. 3(b), is a rectangular structure. Owing to the square shape of this key bar, the stator core can be assembled from the side, which helps to reduce the assembly time. However, a greater penetration depth is required to support the stator core firmly.

III. ANALYSIS

A. MODEL SPECIFICATION

The loss distribution of the generator depends on the generator cooling type. In air-cooled generators, the contribution of mechanical (friction) loss is greater than that in hydrogen-cooled generators because the density of air is greater than that of hydrogen. To compare the effects of key bar types on core loss, generators with the same cooling type and similar capacity were selected, as shown in Table 2.

The generators in this study were of the air-cooled type used in thermal power plants. The rated voltage of both

generators was the same, and the difference in power capacity was approximately 3.05%.

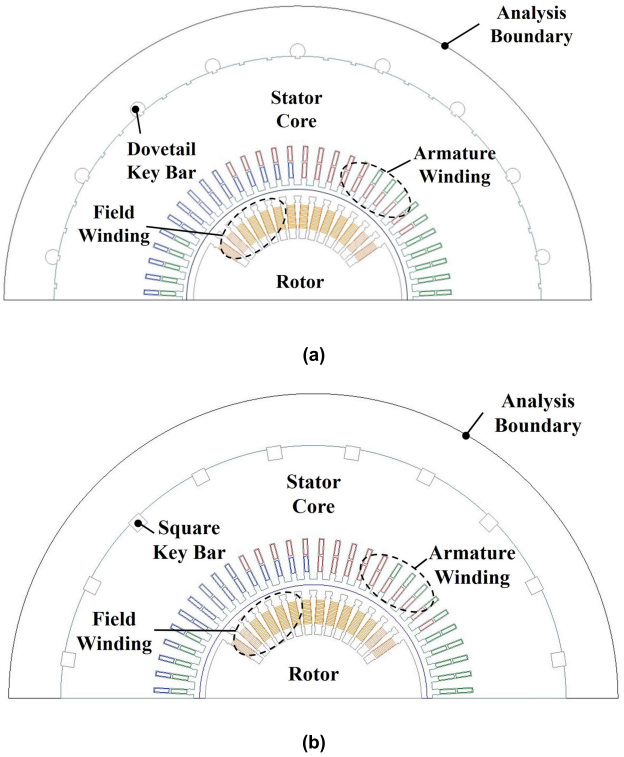

FIGURE 4. Generator model: (a) Dovetail key bar model, (b) Square key bar model.

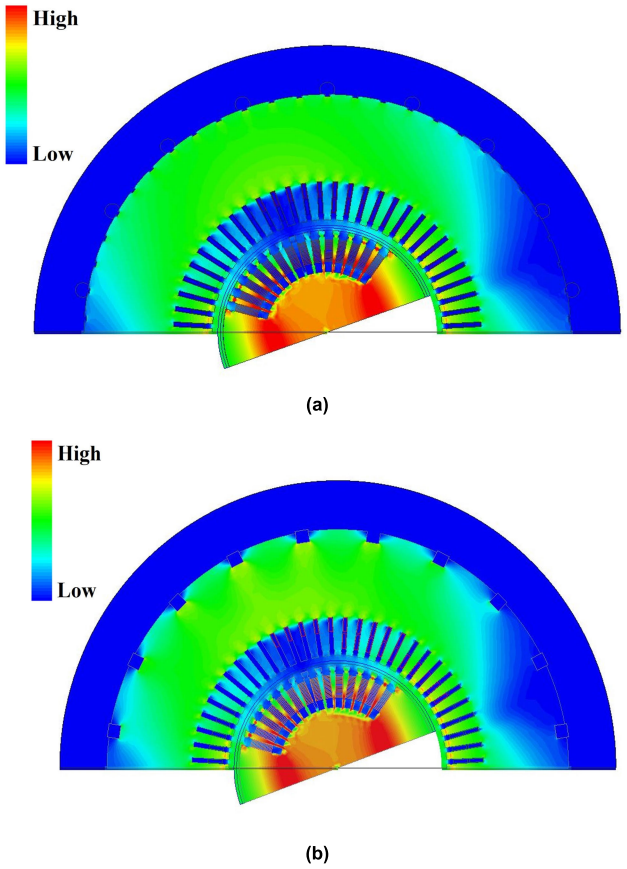

FIGURE 5. Total magnetic flux density distribution: (a) Dovetail key bar model, (b) Square key bar model.

B. FINITE-ELEMENT ANALYSIS MODEL

Fig. 4 shows the FEA model. The analysis was carried out under a no-load open-circuit condition. The terminal voltage was increased from zero to 15 kV in 3 kV increments to replicate the factory-test conditions. The two-pole generators were applied to a 60 Hz system; hence, the rotor and field winding were set to a 3,600 RPM rotational zone. A transient analysis was required to calculate the core loss. We performed a half-model analysis on several cases according to the time flow.

The stator cores in all of the generators were composed of the same material, had the same outer diameter, and the same number and depth of stator core slots. Owing to the difference in capacity, the stator core slot width and armature winding width in the square key bar model were several millimeters larger than those in the dovetail key bar model; nevertheless, the geometries of the rotor and the field winding were the same. Therefore, D1 and S1 in Fig. 6 and Fig. 7 are the same, except for the stator core width and armature winding width.

For each key bar type, we also analyzed the models with and without key bars. By comparing the results of these two analyses, we can determine the extent to which the core loss changes depending on whether the key bar is included. Table 3 shows the analysis cases.

TABLE 3. Analysis cases.

	Dovetail type	Square type
Without key bar	D1	S1
With key bar	D2	S2

C. ANALYSIS RESULTS

Fig. 5, 6, and 7 present the results of the electromagnetic field analysis of the generators in a no-load open-circuit condition. The magnetic flux density is concentrated at the stator core and is low at the key bar, as shown in Fig. 5. This is due to the difference in the relative permeability of the stator core and the key bar. The magnetic flux density (B) is the product of the permeability (u) and magnetic field intensity (H). Permeability is determined by the product of the free space permeability (u_0) and relative permeability (u_r). Thus,

$$B = u \cdot H = u_0 \cdot u_r \cdot H \tag{5}$$

A higher relative permeability indicates a lower magnetoresistance. As shown in Fig. 8, the relative permeability of the stator core is several tens of times larger than that of the key bar over the operation range. Therefore, the magnetic flux from the rotor moves through the stator core, which has a higher permeability.

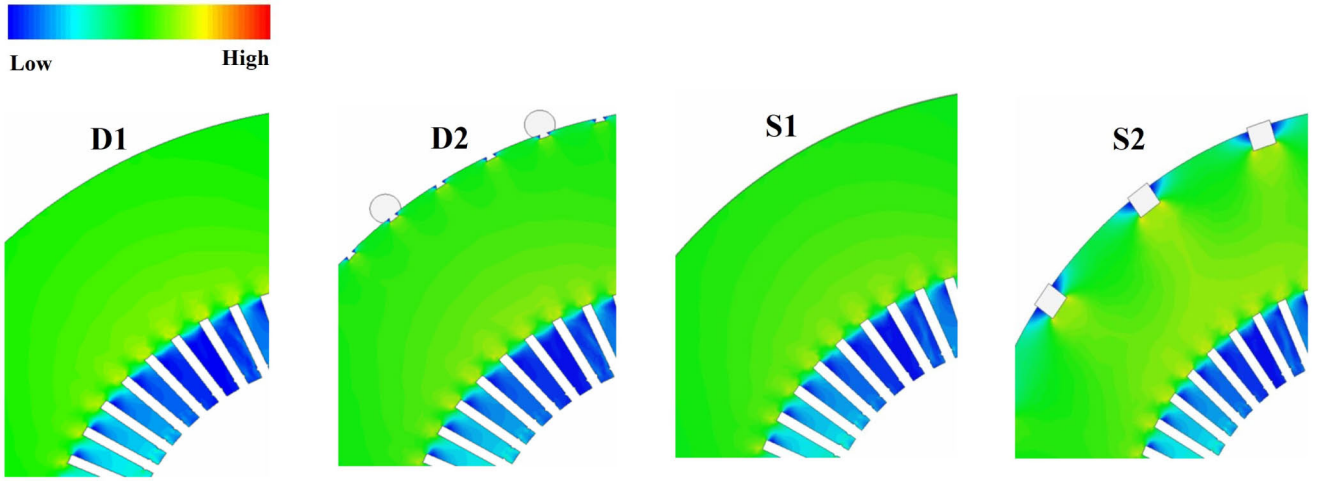

FIGURE 6. Analysis result: Magnetic flux density at the stator core for dovetail (D) and square (S) key bar models, without (1) or with (2) the key bar.

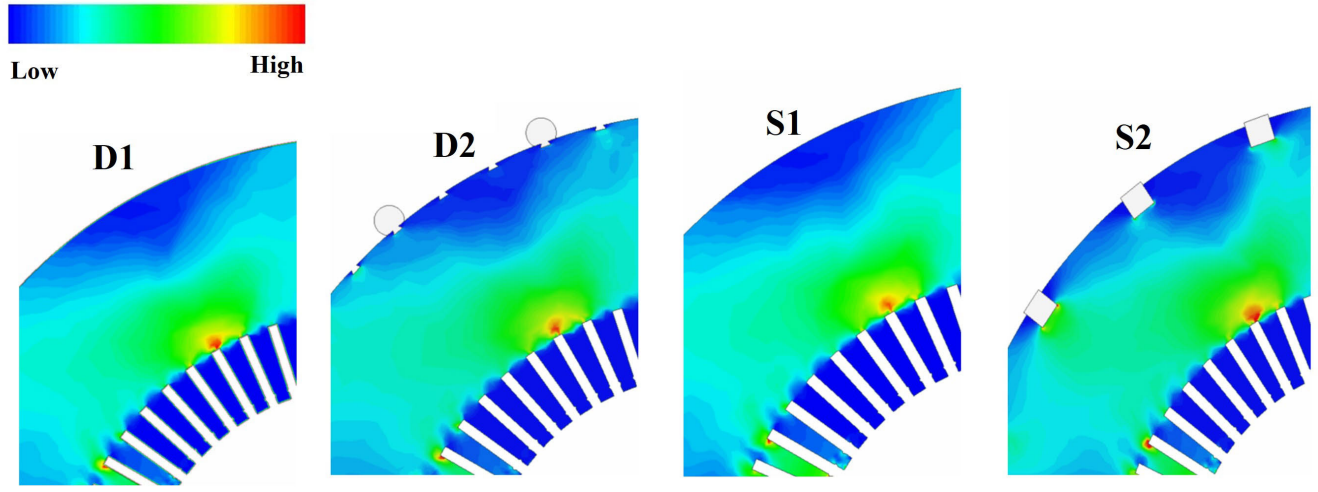

FIGURE 7. Analysis result: Core-loss density at the stator core for dovetail (D) and square (S) key bar models, without (1) or with (2) the key bar.

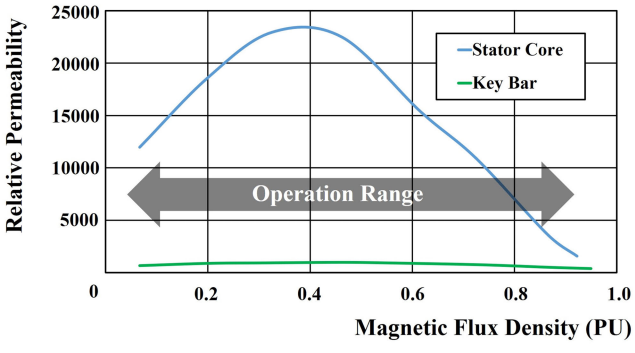

FIGURE 8. Relative permeability of the stator core and the key bar in the operation range.

When the key bar is not included, the magnetic flux density is uniformly distributed up to the outer diameter of the stator core, as shown in Fig. 6 (cases D1 and S1). The core-loss density also extends to the outer diameter of the stator core and is high in the inner region of the stator core, as shown in Fig. 7. The dimensions of the rotor, field winding, and stator core outer diameter and length are the same for the two generators, and the stator core slot widths differ by only a few millimeters. Therefore, without the key bar, the magnetic flux density distribution and core-loss density distribution for the two generators are almost identical, as shown in Fig. 6 and 7 (cases D1 and S1).

With the key bar, the magnetic flux density does not reach the outer diameter of the core and is mainly concentrated between the key bar and the inner diameter of the core, as shown in Fig. 6 (cases D2 and S2). The core-loss density is also high in the region between the key bar and the core inner diameter. This phenomenon is particularly noticeable with the square key bar model, which exhibits deeper penetration.

IV. FACTORY TEST

Generators with a dovetail key bar and a square key bar were manufactured, and factory tests were performed. The core loss in each generator was obtained by the following process:

A. ROLLING TEST

- Test Condition: No current flows through the field winding. The rotor parts rotate at 3,600 RPM.
- Loss Component: Mechanical loss (friction loss) due to the 3,600 RPM rotation.

B. OPEN-CIRCUIT TEST

- Test Condition: Current flows through the field winding, and the open-circuit voltage of the armature winding is measured. The rotor parts rotate at 3,600 RPM.
- Loss Components: Mechanical (friction loss) due to the 3,600 RPM rotation, ohmic loss in the field winding, and core loss in the stator core.

Subtracting the total loss obtained via the rolling test from that obtained via the open-circuit test yields the core loss and the field-winding ohmic loss. The resistance (R_f) of the field winding was measured after manufacturing the generator. Since the field current (I_f) was measured during the generator test, the ohmic loss of the field winding can be calculated as follows:

$$Field - Winding\ Ohmic\ Loss = I_f^2 \cdot R_f \tag{6}$$

Thus, the core loss in the open-circuit condition can be obtained by subtracting the field-winding ohmic loss from the loss-value difference of the two tests. The flow chart of core-loss calculation through the factory test is shown in Fig. 9.

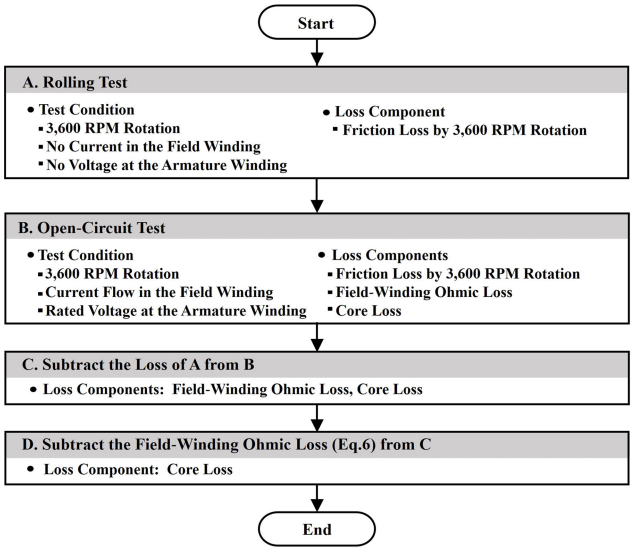

FIGURE 9. Flow chart of the core-loss calculation through factory test.

Each generator was manufactured as shown in Fig. 10 and tested from 0 kV to 15 kV with 3 kV increments in terminal voltage.

V. TEST RESULTS AND DISCUSSION

The analysis and factory-test results for core loss are shown in Fig. 11 and Table 4. Fig. 11 presents the core loss for each case from 0 kV to 15 kV. Table 4 shows the difference in the core loss for each case at the rated voltage relative to the analysis result for the dovetail model without the key bar.

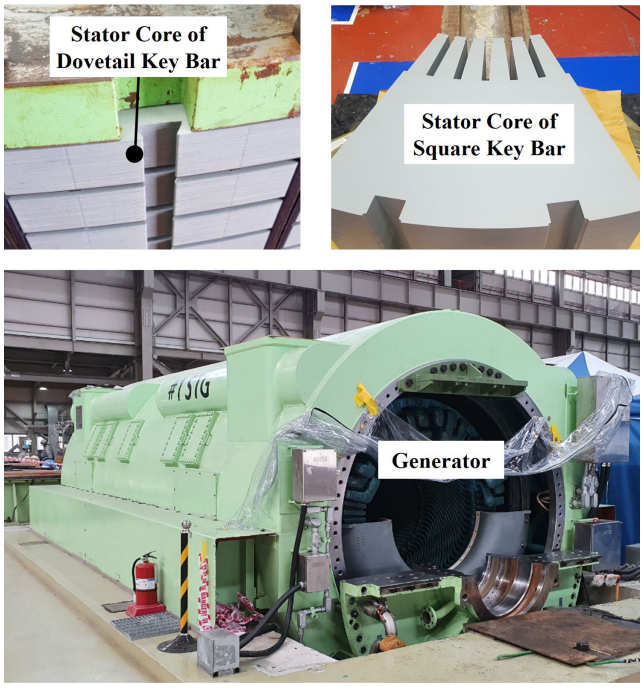

FIGURE 10. Stator cores and factory-test apparatus.

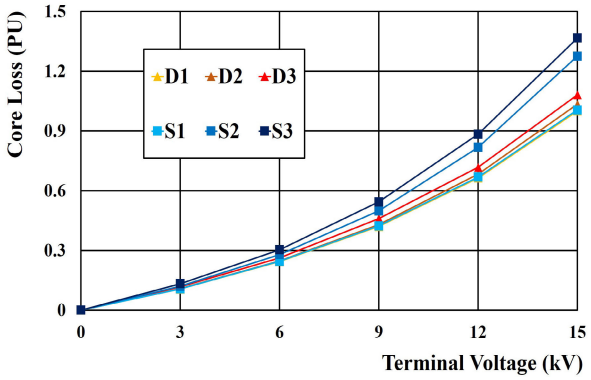

FIGURE 11. Core-loss versus voltage for dovetail (D) and square (S) key bar cases: analysis without key bar (1); analysis with key bar (2); factory test (3).

TABLE 4. Analysis and factory-test results of the core loss at the rated voltage (15 kV).

(Unit: PU)

	Dovetail type	Square type
Analysis result: without key bar	D1: 1.000	S1: 1.005
Analysis result: with key bar	D2: 1.034	S2: 1.275
Factory test	D3: 1.082	S3: 1.367

The model results without the key bar (D1, S1) differ by only 0.5%. This is because the generator dimensions are the same, with the exception of the core slot width. The core slot width of the square type model is a few millimeters larger than that of the dovetail type model.

The difference between the D1 and D2 results is 3.4%. As shown in Figs. 6 and 7, the application of the key bar does not have a significant effect on the changes in the magnetic flux density distribution and the core-loss distribution. This is because the penetration depth of the dovetail key bar into the stator core is small. However, in the case of the square key bar (S1, S2), the results reveal a core-loss difference of 26.8% when the key bar is considered. As can be seen in Figs. 6 and 7, the effective area of the magnetic flux route is reduced by the penetration of the square key bar. Thus, in (3), the width of the stator core (W_{SC}) is reduced, and the magnetic flux density (B_C) is increased. Therefore, the core loss defined in (4) is increased.

By comparing the analysis results and the factory-test results (D2-D3 and S2-S3), we observe that the loss in the factory test was larger by 4.6% for the dovetail key bar and by 7.2% for the square key bar. The difference between the analysis results and factory-test data is caused by eddy-current loss in the key bars, generator-end-region loss owing to magnetic flux leakage [33], and the performance degradation of the stator cores owing to the manufacturing process [29]–[32]. The key bar is made of carbon steel, a conductive material. Eddy-current loss occurs in the key bar under the influence of the magnetic flux flowing to the stator core. However, the majority of the magnetic flux flows through the stator core rather than the key bar, as shown in Fig. 5; consequently, the eddy-current loss of the key bars is small compared to the core loss. Generator stator cores are manufactured using a punching process and assembled into the generator, which is then pressed at both ends; the performance of the stator core decreases due to the mechanical stress. Unlike the dovetail key bar, the square key bar requires a welding process, which results in additional deterioration due to heat. Moreover, the core loss of a generator is calculated for ideal conditions, whereas the actual generator entails deviations arising from manufacturing tolerances that may cause core-loss increases when compared to the losses under ideal analysis conditions.

Summarizing the above results, the core loss differs by 8.2% in the dovetail key bar case (D1-D3) and by 36.0% in the square key bar case (S1-S3).

For the generators in this study, the core loss accounts for 13.5% of total generator losses. Therefore, the total loss increase considering the key bar is 1.1% for the dovetail key bar and 4.8% for the square key bar. The efficiency of a generator is usually above 98% [2], [3], [34]. Hence, an increase of 4.8% of the total loss significantly reduces the competitiveness of the generator. Further, according to the IEEE standard [35], the loss tolerance of a synchronous generator, with a capacity of 10 MVA and above, should be within +10%. Therefore, if a loss difference of 4.8% occurs from the core loss alone, the design criteria may easily be exceeded.

Fig. 12 shows the magnetic flux density and core loss according to key bar type at 12 kV and 15 kV. As the magnetic flux density increases, the core loss rises. The magnetic flux density increases at a certain rate for each key bar type. The core-loss increase is larger at the higher voltage, as shown in Fig. 12. Recently, generators with a high energy and high magnetic flux density have been designed to enable competitive pricing [3]. If factors that affect the stator core, such as the key bar type, are not considered at the design stage, the difference in the efficiency after manufacturing can be significant.

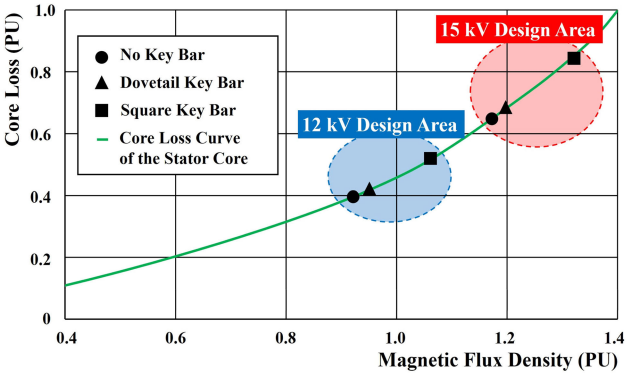

FIGURE 12. Core-loss curve and design points.

VI. CONCLUSION

In this paper, we describe the impact of the key bars used in large turbine generators on core loss. The core losses of a generator with a dovetail key bar and square key bar were calculated by FEA and verified by factory testing.

It was found that the effective area of the magnetic flux route in the stator core is reduced by the penetration of the key bar into the stator core. As a result, the magnetic flux density and core loss are increased.

This increase in the core loss becomes greater in devices with a high magnetic flux density. Therefore, when designing a key bar for a large turbine generator, care must be taken about how deeply the key bar penetrates the stator core.

Furthermore, a generator can be operated continuously under the low frequency (−2%) and high voltage (+5%) condition [35]. In this case, more magnetic flux passes to the stator core as per (2), which increases the core loss according to (4). Therefore, it is necessary to consider that the core loss during actual operation can be higher than that during rated operation.

In energy-conversion devices that use a stator core, such as generators and motors, core loss has a significant impact on performance. Therefore, if there is a structure such as the key bar that affects the stator core, ensuring the performance of the machine requires estimating the core loss at the design stage and then verifying the result by a factory test.

REFERENCES

[1] B. E. B. Gott, "Application of air-cooled generators to modern power plants," in *Proc. IEEE Int. Electr. Drives Conf.*, Seattle, WA, USA, May 1999, pp. 317–319.

[2] S. Nagano, T. Kitajima, K. Yoshida, Y. Kazao, Y. Kabata, D. Murata, and K. Nagakura, "Development of world's largest hydrogen-cooled turbine generator," in *Proc. IEEE Power Eng. Soc. Summer Meeting*, vol. 2, Jul. 2002, pp. 657–663.
[3] Y. Yamamoto, T. Namera, T. Otaka, H. Ito, and M. Tari, "Successful manufacturing and shop testing of the world's largest tandem 2-pole 60 Hz 1000 MW turbine generator," in *Proc. IEEE PES Summer Meeting*, Jul. 2001, pp. 1393–1398.
[4] R. J. Jackson, R. A. Lawrence, and S. R. Rudd, "Refurbishment of turbo-generators for plant life extension," in *Proc. Int. Conf. Refurbishment Power Station Electr. Plant*, London, U.K., 1988, pp. 160–164.
[5] T. Renyuan, X. Guangren, T. Lijian, Z. Danqun, and X. Yi, "Calculation of end region magnetic field and circulation losses for turbo-generators using a coupled field and circuit equations method," *IEEE Trans. Magn.*, vol. 26, no. 2, pp. 497–500, Mar. 1990.
[6] K. Motoyoshi, H. Kometani, N. Sora, and S. Maeda, "Large-scale 3D electromagnetic field analysis for estimation of stator end region loss in turbine generators," in *Proc. 19th Int. Conf. Elect. Mach. Syst. (ICEMS)*, Chiba, Japan, 2016, pp. 1–6.
[7] D. Hiramatsu, T. Tokumasu, M. Fujita, M. Kakiuchi, T. Otaka, O. Sato, and K. Nagasaka, "A study on rotor surface losses in small-to-medium cylindrical synchronous machine," *IEEE Trans. Energy Convers.*, vol. 27, no. 4, pp. 813–821, Dec. 2012.
[8] M. Fujita, T. Hirose, T. Ueda, H. Ishizuka, M. Okubo, K. Nagakura, and T. Tokumasu, "Inter-strand circulating current analysis of end-region transposed coil of power generator using 3D multi-layer FEM," in *Proc. 19th Int. Conf. Elect. Mach. Syst. (ICEMS)*, Chiba, Japan, 2016, pp. 1–6.
[9] J. Han, B. Ge, and W. Li, "Influence of magnetic permeability of the press plate on the loss and temperature of the end part in the end region of a turbogenerator," *IEEE Trans. Ind. Electron.*, vol. 66, no. 1, pp. 162–171, Jan. 2019.
[10] X. Bian and Y. Liang, "Analysis on eddy current losses in stator windings of large hydro-generator considering transposed structure based on analytical calculation method," *IEEE Access*, vol. 7, pp. 163948–163957, 2019.
[11] Y. Liang, L. Wu, X. Bian, and C. Wang, "Influence of void transposition structure on the leakage magnetic field and circulating current loss of stator bars in water-cooled turbo-generators," *IEEE Trans. Ind. Electron.*, vol. 63, no. 6, pp. 3389–3396, Jun. 2016.
[12] G. Traxler-Samek, R. Zickermann, and A. Schwery, "Cooling airflow, losses, and temperatures in large air-cooled synchronous machines," *IEEE Trans. Ind. Electron.*, vol. 57, no. 1, pp. 172–180, Jan. 2010.
[13] Y. Liang, H. Yu, and X. Bian, "Finite-element calculation of 3-D transient electromagnetic field in end region and eddy-current loss decrease in stator end clamping plate of large hydrogenerator," *IEEE Trans. Ind. Electron.*, vol. 62, no. 12, pp. 7331–7338, Oct. 2015.
[14] L. Wang, B. Kou, and W. Cai, "Research on resistance enhancement coefficient and thermal dissipation of stator strands in huge synchronous generator," *IEEE Access*, vol. 8, pp. 40357–40366, 2020.
[15] G. Bertotti, "General properties of power losses in soft ferromagnetic materials," *IEEE Trans. Magn.*, vol. MAG-24, no. 1, pp. 621–630, Jan. 1988.
[16] Y. Chen and P. Pillay, "An improved formula for lamination core loss calculations in machines operating with high frequency and high flux density excitation," in *Proc. Conf. Rec. IEEE-IAS Annual. Meeting*, vol. 2, Oct. 2002, pp. 759–766.
[17] D. Lin, P. Zhou, W. N. Fu, Z. Badics, and Z. J. Cendes, "A dynamic core loss model for soft ferromagnetic and power ferrite materials in transient finite element analysis," *IEEE Trans. Magn.*, vol. 40, no. 2, pp. 1318–1321, Mar. 2004.
[18] A. Balamurali, A. Kundu, Z. Li, and N. C. Kar, "Improved harmonic iron loss and stator current vector determination for maximum efficiency control of PMSM in EV applications," *IEEE Trans. Ind. Appl.*, vol. 57, no. 1, pp. 363–373, Jan. 2021.
[19] D. Zhang, T. Liu, H. Zhao, and T. Wu, "An analytical iron loss calculation model of inverter-fed induction motors considering supply and slot harmonics," *IEEE Trans. Ind. Electron.*, vol. 66, no. 12, pp. 9194–9204, Dec. 2019.
[20] X. Sun, Z. Shi, G. Lei, Y. Guo, and J. Zhu, "Analysis and design optimization of a permanent magnet synchronous motor for a campus patrol electric vehicle," *IEEE Trans. Veh. Technol.*, vol. 68, no. 11, pp. 10535–10544, Nov. 2019.
[21] M. Amin and G. A. A. Aziz, "Hybrid adopted materials in permanent magnet-assisted synchronous reluctance motor with rotating losses computation," *IEEE Trans. Magn.*, vol. 55, no. 6, pp. 1–5, Jun. 2019.
[22] M. Fratila, A. Benabou, A. Tounzi, and M. Dessoude, "Iron loss calculation in a synchronous generator using finite element analysis," *IEEE Trans. Energy Convers.*, vol. 32, no. 2, pp. 640–648, Jun. 2017.
[23] P. A. Hargreaves, B. C. Mecrow, and R. Hall, "Calculation of iron loss in electrical generators using finite-element analysis," *IEEE Trans. Ind. Appl.*, vol. 48, no. 5, pp. 1460–1466, Sep./Oct. 2012.
[24] M. Ranlof, A. Wolfbrandt, J. Lidenholm, and U. Lundin, "Core loss prediction in large hydropower generators: Influence of rotational fields," *IEEE Trans. Magn.*, vol. 45, no. 8, pp. 3200–3206, Aug. 2009.
[25] R. Romary, C. Demian, P. Schlupp, and J.-Y. Roger, "Offline and online methods for stator core fault detection in large generators," *IEEE Trans. Ind. Electron.*, vol. 60, no. 9, pp. 4084–4092, Sep. 2013.
[26] A. C. Smith, D. Bertenshaw, C. W. Ho, T. Chan, and M. Sasic, "Detection of stator core faults in large turbo-generators," in *Proc. IEEE Int. Electric Mach. Drives Conf. (IEMDC)*, Miami, FL, USA, May 2009, pp. 763–770.
[27] S. B. Lee, G. B. Kliman, M. R. Shah, N. K. Nair, and R. M. Lusted, "An iron core probe based inter-laminar core fault detection technique for generator stator cores," *IEEE Trans. Energy Convers.*, vol. 20, no. 2, pp. 344–351, Jun. 2005.
[28] D.-I. Song and J. Lee, "Electromagnetic field analysis of the dovetail key bar voltage in a generator," *J. Korean Phys. Soc.*, vol. 76, no. 8, pp. 757–761, Apr. 2020.
[29] R. Sundaria, A. Lehikoinen, A. Arkkio, and A. Belahcen, "Effects of manufacturing processes on core losses of electrical machines," *IEEE Trans. Energy Convers.*, vol. 36, no. 1, pp. 197–206, Mar. 2021.
[30] A. J. Clerc and A. Muetze, "Measurement of stator core magnetic degradation during the manufacturing process," *IEEE Trans. Ind. Appl.*, vol. 48, no. 4, pp. 1344–1352, Jul. 2012.
[31] A. Schoppa, J. Schneider, and C.-D. Wuppermann, "Influence of the manufacturing process on the magnetic properties of non-oriented electrical steels," *J. Magn. Magn. Mater.*, vols. 215–216, pp. 74–78, Jun. 2000.
[32] A. Schoppa, J. Schneider, C.-D. Wuppermann, and T. Bakon, "Influence of welding and sticking of laminations on the magnetic properties of non-oriented electrical steels," *J. Magn. Magn. Mater.*, vols. 254–255, pp. 367–369, Jan. 2003.
[33] S. Li, C. Gong, L. Du, J. R. Mayor, R. G. Harley, and T. G. Habetler, "Parametric study for the design of the end region of large synchronous generators based on three-dimensional transient finite element analysis," in *Proc. IEEE Energy Convers. Congr. Expo. (ECCE)*, Sep. 2018, pp. 7356–7362.
[34] Y. Taniyama, T. Ueda, M. Fujita, T. Okamoto, M. Arata, H. Katayama, K. Nagakura, and T. Otaka, "Technologies for high efficiency large capacity turbine generator," in *Proc. Int. Conf. Electr. Mach. Syst.*, Nov. 2009, pp. 1–6.
[35] *IEEE Standard for Cylindrical-Rotor 50Hz and 60 Hz Synchronous Generators Rated 10 MVA and Above*, IEEE Standard C50.14, IEEE Power and Energy Society, 2014.

DAE-IL SONG received the B.S. degree in electrical and computer engineering from Hanyang University, Seoul, South Korea, in 2010, and the M.S. degree in electrical engineering from the Korea Advanced Institute of Science and Technology (KAIST), Daejeon, South Korea, in 2012. He is currently pursuing the Ph.D. degree with the Department of Electrical Engineering, Hanyang University. From 2011 to 2019, he worked with the Generator Development Team, Doosan Heavy Industry, Changwon, South Korea. Since 2019, he has been working with the Power Generation Laboratory, Korea Electric Power Research Institute (KEPRI), Daejeon. His current research interests include development to improve the performance and reliability of large turbine generators and synchronous condensers.

JUNGHWAN AHN received the B.A. and Ph.D. degrees in electrical engineering from Hanyang University, Seoul, South Korea, in 2013 and 2018, respectively. Since 2019, he has been working with the Korea Electric Power Research Institute (KEPRI), Daejeon, South Korea. His current research interests include status diagnosis and optimization of power facilities.

YOUNG-JOON NAM received the M.S. degree in electrical engineering from Hanyang University, Seoul, South Korea, in 2016, where he is currently pursuing the Ph.D. degree with the Department of Electrical Engineering. He is responsible for research and development, as the CTO of Coslight, South Korea. His main research interest includes the storage and conversion of electrical energy.

JU LEE (Senior Member, IEEE) received the B.S. and M.S. degrees from Hanyang University, Seoul, South Korea, in 1986 and 1988, respectively, and the Ph.D. degree from Kyushu University, Japan, in 1997, all in electrical engineering. In 1997, he joined Hanyang University, where he is currently a Professor with the Division of Electrical and Biomedical Engineering. His main research interests include electric machinery and drives, electromagnetic field analysis, and transportation systems, such as hybrid electric vehicles and railway propulsion systems. He is a member of the IEEE Industry Applications Society, the Magnetics Society, and the Power Electronics Society.

HYUNGKWAN JANG received the B.S. and M.S. degrees in electrical engineering from Hanyang University, Seoul, South Korea, in 2010 and 2012, respectively. He is currently pursuing the Ph.D. degree in electrical engineering. From 2013 to 2017, he worked with LG Electronics. His research interests include the design and analysis of motors/generators, and the applications of mechanical and electrical systems in railway cars, electric vehicles, automotive parts, and home appliances.